WATER RESOURCES RESEARCH, VOL. 49, 1–15, doi:10.1002/wrcr.20396, 2013

Combining fixed- and moving-vessel acoustic Doppler current profiler measurements for improved characterization of the mean flow in a natural river

John Petrie,[1] Panayiotis Diplas,[2] Marte Gutierrez,[3] and Soonkie Nam[4]

Received 14 March 2013; revised 13 June 2013; accepted 1 July 2013.

[1] A methodology is presented to quantify the mean flow field in a natural river with a boat-mounted acoustic Doppler current profiler (ADCP). Moving-vessel (MV) and fixed-vessel (FV) survey procedures are used in a complementary fashion to provide an improved representation of mean three-dimensional velocity profiles along a cross section. Mean velocity profiles determined with FV measurements are rotated to a stream-fitted orthogonal coordinate system. The orientation of the coordinate system is established using MV measurements. The methodology is demonstrated using measurements obtained at two study sites on the lower Roanoke River for the mean annual flow (228 m^3 s^{-1}) and a flow that produces bankfull conditions at the sites (565 m^3 s^{-1}). Results at a meander bend identify well-known flow features, including a main circulation cell, outer-bank circulation, and separation at the inner bank. This methodology also provides a framework for comparing time-averaged velocity profiles from FV measurements with spatially averaged profiles from MV measurements. Results indicate that MV measurements can provide a reasonable estimate of the streamwise velocity at many locations. The MV measurements obtained here, however, were not sufficient to resolve the spanwise velocity component.

Citation: Petrie, J., P. Diplas, M. Gutierrez, and S. Nam (2013), Combining fixed- and moving-vessel acoustic Doppler current profiler measurements for improved characterization of the mean flow in a natural river, *Water Resour. Res.*, *49*, doi:10.1002/wrcr.20396.

1. Introduction

[2] The flow field in natural rivers is characterized by turbulent three-dimensional (3-D) velocity. The 3-D nature of velocity is due to channel planform curvature and pronounced channel topography [e.g., *Rozovskii*, 1957; *Dietrich and Smith*, 1983] as well as anisotropic turbulence [*Tominaga et al*., 1989]. To interpret field data, velocity measurements are often decomposed into orthogonal components in the streamwise, spanwise, and vertical directions. Orientation of the horizontal components is dependent on the definition of the primary flow direction. Typically, the streamwise flow direction is prescribed using either channel geometry or flow characteristics. Velocity components in the plane perpendicular to the streamwise direction formed by the spanwise and vertical axes are referred to as secondary velocities and are known to influence channel morphology [e.g., *Blanckaert*, 2011] and ecology [e.g., *Shen and Diplas*, 2008, 2010]. Interpretation of secondary velocity patterns is complicated due to the small magnitudes relative to the streamwise component as well as when only the horizontal velocity is measured and vertical velocity must be inferred. *Lane et al*. [2000] advocated the use of 3-D computational fluid dynamics (CFD) models to directly represent velocity vectors as an alternative to interpreting orthogonal components. Flows in natural rivers are particularly challenging to model due to the presence of moving boundaries, including both the channel boundary and free-surface, complex topography, turbulence, and boundary roughness. Despite these complexities, CFD has been applied to flows in natural rivers with promising results [e.g., *Ferguson et al*., 2003; *Shen and Diplas*, 2008, 2010; *Rüther et al*., 2010]. High-resolution field data for boundary conditions and validation are needed to support the expanding role of CFD in fluvial hydraulics.

[3] A boat-mounted acoustic Doppler current profiler (ADCP) is a versatile tool for riverine studies that can provide measurements of 3-D velocity and channel topography. The spatial and temporal resolution of the velocity measurements is dependent on the type of deployment. During moving-vessel (MV) measurements, the ADCP records continuously while the boat traverses the channel. This is the most common boat-mounted survey procedure and provides accurate measurements of discharge [*Oberg and Mueller*, 2007]. Fixed-vessel (FV) measurements are performed while the boat is held at a constant position

[1]Department of Civil and Environmental Engineering, Washington State University, Pullman, Washington, USA.
[2]Imbt Environmental Hydraulics Laboratory, Department of Civil and Environmental Engineering, Lehigh University, Bethlehem, Pennsylvania, USA.
[3]Division of Engineering, Colorado School of Mines, Golden, Colorado, USA.
[4]Department of Civil and Environmental Engineering, South Dakota School of Mines and Technology, Rapid City, South Dakota, USA.

Corresponding author: J. Petrie, Department of Civil and Environmental Engineering, Washington State University, 405 Spokane St., Sloan 101, Pullman, WA 99164-2910, USA. (j.petrie@wsu.edu)

0043-1397/13/10.1002/wrcr.20396

within the channel. The improved temporal resolution can be used to determine mean (e.g., time-averaged) velocity profiles [*Petrie et al*., 2013] and bed load velocity [*Rennie et al*., 2002]. Due to the increased effort required to collect FV measurements, several studies have investigated mean velocity profiles from MV measurements using spatial averaging or interpolation [*Muste et al*., 2004a, 2004b; *Dinehart and Burau*, 2005; *Szupiany et al*., 2007]. Recently, kriging has been used to interpolate planform maps of flow quantities, including depth-averaged velocity, boundary shear stress, and bed load velocity, from MV measurements [*Rennie and Church*, 2010; *Guerrero and Lamberti*, 2011]. *Jamieson et al*. [2011] and *Tsubaki et al*. [2012] have extended this work to interpolate the 3-D velocity field. While these maps do not represent mean quantities in a strict time-averaged sense, *Jamieson et al*. [2011] argued that interpolated maps may better represent a complex flow field than averaging repeat transects that are not coincident and introduce spatial averaging. Nonetheless, a detailed comparison of interpolated maps to time-averaged velocities has yet to be reported.

[4] This study presents a methodology to quantify the mean flow field in a natural river with a boat-mounted ADCP using both MV and FV survey procedures. This approach capitalizes on the relative advantage of each procedure, with the MV measurements providing the direction of primary flow and channel topography while the FV measurements determine the mean velocity profiles. A comparison of mean velocity profiles from FV and MV measurements is performed to determine if the MV measurements can quantify the spatial distribution of the mean secondary velocity. The methodology is then demonstrated by examining mean velocity profiles throughout a meander bend.

2. Field Measurements

2.1. Study Sites

[5] ADCP measurements were obtained in May and June 2009 at two study sites shown in Figure 1 on the lower Roanoke River in eastern North Carolina. Flow to the lower reach is primarily controlled by releases from the Roanoke Rapids Dam. The effect of this flow regulation on bank retreat has been the subject of recent investigations [*Hupp et al*., 2009; *Nam et al*., 2010, 2011]. Reservoir releases were relatively steady for both survey periods, with the discharge Q in May close to the mean annual flow ($Q = 228$ m^3 s^{-1}) and at bankfull in June ($Q = 565$ m^3 s^{-1}). Further information on the study sites and flow conditions is provided in *Petrie et al*. [2013].

2.2. Equipment and Measurement Procedures

[6] The ADCP measures 3-D velocity components by applying the Doppler principle to the frequency shift of reflected acoustic pulses, called pings. Measurements are assigned to equally spaced discrete locations in the water column, called bins. A bin size of 0.25 m was used for all measurements in this study. Limitations of the instrument prevent velocity measurements from being obtained near the water surface or near the bed [see *Simpson*, 2001]. An ensemble is one measurement of the velocity profile and may be composed of a single ping or the average of several pings. For the FV measurements, 20 subpings sent 50 ms apart were used to create each ensemble. The recommended settings provided by the ADCP software were used for the MV measurements. For the mean annual flow, this resulted in seven subpings sent 40 ms apart to create an ensemble for most transects and one subping sent 70 ms apart for most transects during the bankfull flow. Data were collected using Water Mode 12 and Bottom Mode 5 [see *Mueller and Wagner*, 2009]. Global positioning system (GPS) was used as the velocity reference for all measurements, with the exception of one FV measurement, S1xs6p2 (nomenclature is explained in the following section), during the mean annual flow, due to a problem with the GPS signal. The decision to use GPS was based on observations of bed movement, especially during the bankfull flow. Further details on ADCP operational principles can be found in the work of *Gordon* [1989], *Simpson* [2001], and *Mueller and Wagner* [2009].

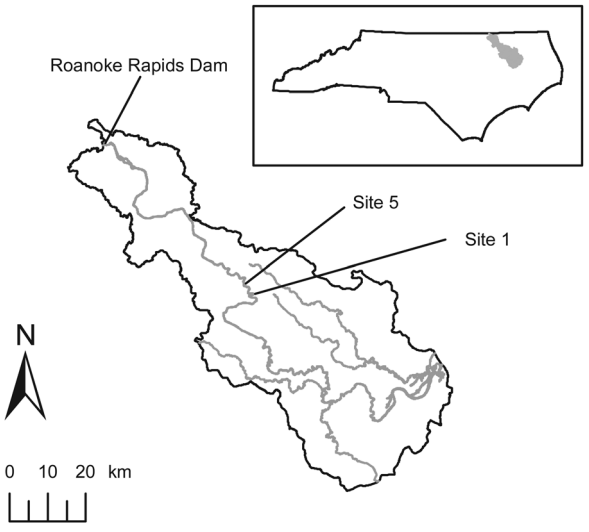

Figure 1. Map of the portion of the lower Roanoke River watershed located within North Carolina. The location of the watershed in North Carolina is shown in gray in the box [from *Petrie et al*., 2013].

[7] A 1200 kHz Workhorse Rio Grande ADCP (Teledyne RD Instruments, Poway, CA) and a Trimble DSM 232 GPS (Sunnyvale, CA) were mounted to a tethered boat (Oceanscience, Oceanside, CA). The GPS antenna is positioned directly above the ADCP at a height of about 50 cm from the water surface. Rope was used to attach the tethered boat (length = 1.2 m) to the starboard (right) side of a motorboat (length = 6 m). The tethered boat remained on the starboard side near center of the motorboat for both survey procedures. The ADCP and GPS data were recorded with WinRiver II software provided by the ADCP manufacturer. The horizontal accuracy of the GPS was approximately 1.0 m. Measurement locations were found during deployment with HYPACK LITE (HYPACK, Inc., Middletown, CT).

[8] Both MV and FV survey procedures were performed at each study site. FV measurements were performed by anchoring the boat within the channel and measuring continuously for 1200 s. A data assurance procedure was performed on each individual measurement to verify that the

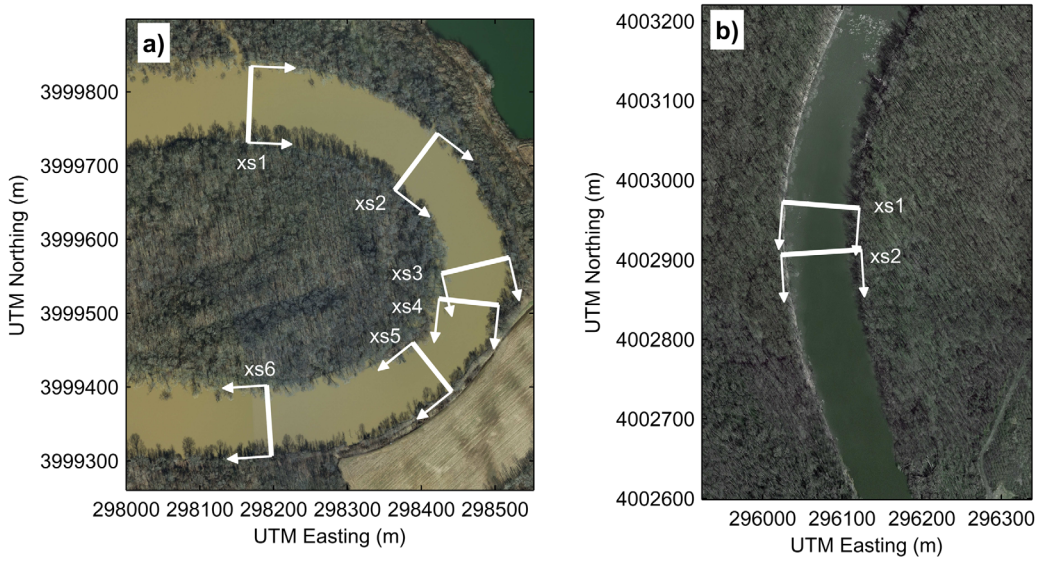

Figure 2. Orientation of the streamwise and spanwise axes using the Paice definition at each cross section during the bankfull flow for (a) Site 1 and (b) Site 5.

measured velocity was (1) statistically stationary, (2) not adversely influenced by motion of the ADCP, and (3) of sufficient sample record length [*Petrie et al*., 2013]. MV measurements consisted of driving the boat from one bank edge to the other in a path approximately perpendicular to the flow direction with the ADCP measuring continuously. One pass across the river produces a single measurement and is referred to as a transect. Four transects, two starting at each bank, were performed at each cross section of interest. Directional errors were observed near the end of some transects as a result of acceleration due to the ADCP turning near the bank edge. The affected ensembles were removed from the sample record.

[9] Measurements were aligned along cross sections, six at Site 1 and two at Site 5, oriented approximately perpendicular to the riverbanks. The cross sections are numbered consecutively from upstream to downstream, as shown in Figure 2. For each discharge, between three and five FV measurements were performed, followed by four MV transects at each cross section. Difficulty positioning the ADCP prevented measurements from occurring at the exact same locations during June 2009. The average distance between the FV locations for the two discharges is 5.1 m. Each FV measurement is labeled to identify the site, cross section, and profile number, e.g., S1xs1p1, where the profile nearest the left bank is designated profile number 1. A total of 25 (26) profiles were measured during the mean annual flow (bankfull flow) at Site 1, and eight profiles were obtained at Site 5 for each discharge. The surveys required approximately 6 days with a three-person crew. Data processing for both FV and MV measurements was performed with in-house codes developed in MATLAB® (The MathWorks, Natick, MA) at the Baker Environmental Hydraulics Laboratory of Virginia Tech.

3. Data Analysis

[10] Interpreting flow data in a natural river can be difficult due to complex channel topography and the turbulent, 3-D nature of velocity. A methodology is presented here that allows velocity data obtained with MV and FV survey procedures to be presented in a consistent framework. The velocity data are first rotated to a common coordinate system and then translated to a two-dimensional plane representing a cross section. This procedure allows a comparison of measured velocity from different survey procedures as well as a hybrid approach to presenting velocity patterns at a cross section, e.g., using the MV measurements to quantify the channel bathymetry and FV measurements to determine mean velocity profiles.

[11] Velocity components are presented in a stream-based coordinate system. As the orientation of the coordinate system may not be known prior to field measurements, ADCP velocity data are output in a Cartesian coordinate system defined by east, E, north, N, and vertical, Z, axes, more specifically the Universal Transverse Mercator (UTM) geographic coordinate system, referred to here as the geographic coordinate system. The geographic components are rotated in the horizontal plane by an angle, α, to the stream coordinate system—a "channel-fitted" curvilinear coordinate system defined by streamwise, s, spanwise, n, and vertical, z, axes. The angle of rotation, α, is measured clockwise from the N axis to the s axis. Representing velocity in stream coordinates allows the velocity vectors to be decomposed into a primary component, oriented along the s axis, and secondary components, occurring within the secondary plane—the plane formed by the n and z axes. The angle of rotation, α, is referred to as the direction of primary flow, the streamwise direction, or simply the flow direction.

[12] The direction of primary flow may be defined using channel geometry or flow characteristics [*Hey and Rainbird*, 1996; *Lane et al*., 2000]. Channel curvature referenced to either the bank edge or channel centerline has been used to define the flow direction in curved laboratory channels [*De Vriend*, 1979; *Blanckaert and Graf*, 2001] as well as field sites [*Dinehart and Burau*, 2005; *Nanson*,

2010; *Sukhodolov*, 2012]. Difficulties may be encountered when applying this approach to natural rivers, including problems identifying the bank edge or channel centerline, nonuniformity between the right and left bank edges, changing channel curvature, and other complex features such as bifurcations and confluences. Definitions using flow characteristics to determine flow direction depend on the spatial extent over which the flow direction is defined with 1-D, 2-D, and 3-D approaches being available. The most commonly applied definition is the one-dimensional approach of *Rozovskii* [1957], where the direction of primary flow along a vertical profile is defined as the direction that results in a zero net secondary discharge across the vertical. Requiring a zero net secondary discharge ensures that both positive and negative spanwise velocity values exist in all profiles. The Rozovskii definition is applied to individual velocity profiles; thus, it provides a local flow direction which may vary for different locations along a cross section. *Paice* [1990] defined the direction of primary flow as the direction that results in the maximum discharge through a vertically oriented plane, a two-dimensional approach. Equivalently, this definition results in zero net secondary discharge in the cross-section plane. The Paice definition produces a single flow direction for a cross section, allowing for regions of unidirectional spanwise velocity to exist.

[13] The choice of definition for the flow direction will influence the interpretation of secondary velocity and depends on the available data. For example, the local flow direction resulting from the Rozovskii definition may obscure flow features when secondary profiles are viewed along a cross section [*Dietrich and Smith*, 1983]. The Paice definition was selected due to the fact that it provides a consistent flow direction along a cross section. The algorithm for computing the flow direction using the Paice definition [see *Hey and Rainbird*, 1996] can be adapted to MV transects using the following steps:

[14] 1. Perform a MV transect in the same manner as obtaining a discharge measurement.

[15] 2. Calculate the streamwise and spanwise velocity components in each bin for all possible angles of rotation from 0° to 360°.

[16] 3. For each angle of rotation, compute the net spanwise discharge for the transect.

[17] 4. The angle of rotation in step 3 which produces a zero net spanwise discharge is the direction of primary flow, α.

[18] Both *Paice* [1990] and *Markham and Thorne* [1992] applied a similar procedure after collecting velocity profiles along a cross section with a current meter and applying the midsection method to compute discharge. MV transects with a boat-mounted ADCP provide spatial resolution of velocity that produce improved estimates of discharge and, likely, the flow direction as well. Calculating discharge in the streamwise and spanwise directions from MV measurements requires a modification to the standard discharge equation presented in *Christensen and Herrick* [1982] and used in WinRiver II. Modification is necessary due to the fact that the standard discharge equation computes the total net horizontal discharge independent of coordinate system [*Simpson*, 2001]. Reintroducing the dependence on coordinate system results in the following equation for the spanwise discharge for the *i*th ensemble:

$$Q_{ni} = \sum_{j=1}^{m} u_{nj} (V_s)_i \Delta t_i \Delta z, \tag{1}$$

where the ensemble contains $j = 1, 2, \ldots, m$ bins; u_{nj} is the spanwise velocity component of the jth bin; $(V_s)_i$ is the streamwise component of the boat velocity for the ensemble; Δt_i is the time elapsed between ensembles i and $i-1$; and Δz is the bin height. Summing over all ensembles provides the total discharge in the spanwise direction:

$$Q_n = \sum_{i=1}^{k} Q_{ni}, \tag{2}$$

where the transect contains $i = 1, 2, \ldots, k$ ensembles. A derivation of equations (1) and (2) is provided in Appendix A. As with discharge measurements [see *Mueller and Wagner*, 2009], multiple transects should be obtained at each cross section and the flow direction computed from the average of the individual transect results.

[19] To present the velocity component in a single plane, velocity data are translated onto the secondary plane. *Dinehart and Burau* [2005] referred to this procedure as "section straightening." While care is taken to obtain measurements close to the cross section, measurements will inevitably vary in location. Multiple MV transects will not be coincident due to difficulty keeping the boat moving along the same straight path while traversing the river channel. Likewise, difficulty fixing the boat at an exact location in the river may prevent the FV measurement locations from lying along the MV transects. *Dinehart and Burau* [2005] defined the horizontal orientation of the plane by fitting a mean line through multiple boat paths, then rotating the ADCP data about a distant point onto the mean line with cosine rotation. It is not explicitly stated how the mean line is fit through the boat paths. Two options are to visually estimate the mean line or perform a linear regression on the horizontal locations from the boat path, as discussed by *Szupiany et al*. [2007].

[20] Following the general approach of *Dinehart and Burau* [2005] and *Szupiany et al*. [2007], the procedure for section straightening presented here fits a straight line through the boat paths of the MV transects. The slope of this line is prescribed to produce a line coincident to the spanwise axis, n, in local stream coordinates. The motivation for using the orientation of the spanwise axis is to provide a convenient physical interpretation for velocity data visualized in the secondary plane. Specifically, when mean spanwise and vertical velocity components are plotted, the resulting patterns occur within the plane as shown. Once the direction of primary flow is determined, section straightening is performed with the following steps.

[21] 1. Rotate the location of all ensembles from MV transects from geographic to stream coordinates.

[22] 2. Translate the MV locations to a local stream coordinate system where the location of the spanwise axis ($s = 0$) is set to the location of the average streamwise location. The location of the primary axis ($n = 0$) is set to the mean of the spanwise locations to approximate the channel centerline.

[23] 3. Translate the locations of MV or FV data perpendicularly to lie on the secondary plane. Following *Dinehart*

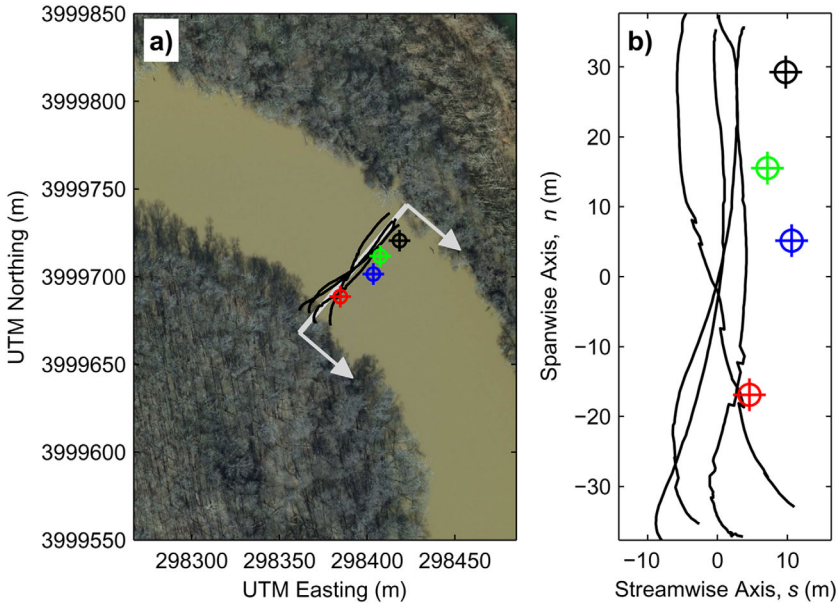

Figure 3. Locations of MV transects (black lines) and FV profiles (targets) at S1xs2 during the mean annual flow in (a) geographic coordinates and (b) stream coordinates. The profiles locations are shown in color: S1xs2p1 (black), S1xs2p2 (green), S1xs2p3 (blue), and S1xs2p4 (red).

and Burau [2005], the translated velocity data remain unchanged.

[24] Once section straightening is performed, any location may be presented in either geographic or stream coordinates. As the stream coordinate system changes for each cross section, geographic coordinates are preferred when representing data from multiple cross sections. Figure 3 demonstrates section straightening for S1xs2 during the mean annual flow. In Figure 3a, the gray line shows the location of the spanwise axis, and the vector arrows indicate the direction of primary flow. Figure 3b shows the FV and MV measurement locations in stream coordinates. The distance required to translate each FV profile to the secondary plane is provided in Table 1. The mean and maximum translation distances for the mean annual flow (bankfull flow) are 7.7 m (8.8 m) and 17.4 m (20.1 m), respectively.

4. Results

4.1. Mean Velocity Profiles From MV and FV Procedures

[25] While time-averaged velocity profiles cannot be directly determined from MV transects, spatial averaging of multiple transects has been used to produce mean profiles [*Dinehart and Burau*, 2005; *Szupiany et al.*, 2007]. The data set from the lower Roanoke River is used to evaluate the adequacy of spatially averaged velocity profiles derived from MV transects to represent mean (i.e., time-averaged) velocity profiles. The velocity profiles from the MV transects at a cross section are compared with time-averaged velocity profiles from FV measurements obtained along the cross section. Mean velocity profiles were obtained from multiple transects by first applying the section-straightening procedure to the individual transects. Each geographic velocity component is interpolated at locations corresponding to the bins in the FV measurement of interest, resulting in a velocity profile for each transect. The velocity profiles interpolated from the individual transects are then averaged to create the mean velocity profile. A similar procedure was employed by *Dinehart and Burau* [2005] to represent secondary velocity components. To provide a consistent coordinate system for comparison, the mean geographic velocity components are rotated using the flow direction determined with the Rozovskii definition from the corresponding FV measurement. The results at two locations are excluded from this analysis: (1) S1xs4p5 for the mean annual flow, which is located in a recirculation region, and (2) S1xs5p5 for the bankfull flow due to the fact that the FV measurement location falls outside of the transects.

[26] The FV and MV results for the streamwise and spanwise velocity components for all bins are compared in Figure 4. Generally, closer agreement is seen in the streamwise component. The majority of bins which show large spanwise velocity from the MV results occur in four profiles: S1xs2p1, S1xs4p1, S1xs4p2, and S1xs4p4 during the mean annual flow. The velocity components at these locations are shown in gray in Figure 4. Example velocity profiles from FV and MV measurements along S5xs1 during the bankfull flow are provided in Figure 5. Reasonable agreement is seen in the streamwise velocity profiles, while the spanwise profiles show differences in both magnitude and direction. The time averaging performed for the FV measurements reduces the effects of instrument noise and turbulent fluctuations, resulting in smoother velocity distributions.

[27] Table 2 presents the mean percent difference and the maximum percent difference between the MV and FV results for each profile of velocity magnitude and streamwise velocity. The median value of the mean percent difference for all profiles is about 10% or less, demonstrating that MV transects can provide reasonable estimates of the

Table 1. Summary of FV Velocity Profiles

		Mean Annual Flow				Bankfull Flow			
		U (m s^{-1})	H (m)	Rozovskii Flow Direction (°)	Translation Distance (m)	U (m s^{-1})	H (m)	Rozovskii Flow Direction (°)	Translation Distance (m)
S1xs1	p1	0.52	5.1	92.5	7.1	0.86	7.7	92.9	6.9
	p2	0.65	4.7	95.7	9.2	0.99	7.3	94.0	0.6
	p3	0.63	4.6	91.8	6.3	0.92	7.3	95.2	0.6
S1xs2	p1	0.71	6.4	131.2	9.8	0.90	9.5	132.5	15.6
	p2	0.66	5.7	134.1	7.2	1.01	9.0	130.5	13.9
	p3	0.68	4.9	132.3	10.6	0.96	8.3	133.0	15.3
	p4	0.70	3.5	125.7	4.6	0.99	6.7	129.7	12.6
S1xs3	p1	0.46	5.7	173.8	8.8	0.73	9.9	167.5	10.5
	p2	0.64	8.3	166.7	8.3	0.99	11.4	170.6	15.2
	p3	0.68	5.8	166.0	6.2	1.00	9.2	168.3	10.9
	p4	0.56	4.6	167.1	1.7	0.88	7.6	167.1	1.0
	p5	0.21	2.2	162.2	9.3	0.69	5.2	161.2	11.1
S1xs4	p1	0.44	6.2	227.8	8.1	0.89	5.8	198.1	17.3
	p2	0.51	11.0	232.4	8.2	0.92	12.2	206.0	18.2
	p3	0.58	13.5	190.0	13.7	0.88	16.7	196.7	20.1
	p4	0.48	11.8	188.0	8.9	0.82	13.7	185.9	14.1
	p5	−0.02	7.8	77.3	5.2	0.52	11.0	187.4	12.4
S1xs5	p1	0.48	4.5	221.7	15.1	0.54	5.4	222.3	9.0
	p2	0.57	8.7	223.3	16.7	0.91	12.0	228.9	3.2
	p3	0.56	7.1	227.2	16.4	0.88	10.3	231.9	13.3
	p4	0.57	5.2	227.1	17.4	0.79	8.2	236.3	5.9
	p5	0.41	3.8	228.9	8.3	0.47	5.4	233.9	11.2
S1xs6	p1	0.75	7.0	256.9	2.5	1.06	10.5	268.2	0.2
	p2	0.61	5.5	257.8	14.6	0.98	7.8	266.8	8.8
	p3	0.61	4.0	260.7	1.5	0.87	7.2	267.9	4.4
	p4	—	—	—	—	0.70	6.2	265.9	5.4
S5xs1	p1	0.61	3.2	177.9	4.3	0.69	6.3	180.3	2.9
	p2	0.72	3.3	183.2	1.0	0.89	7.0	185.4	0.7
	p3	0.65	4.0	180.5	3.9	0.94	7.4	186.6	4.7
	p4	0.71	4.7	180.1	10.2	0.81	8.1	182.8	9.5
S5xs2	p1	0.57	3.2	174.8	0.7	0.72	6.4	176.3	3.6
	p2	0.65	3.5	174.9	0.4	0.86	6.9	176.2	4.9
	p3	0.72	4.0	173.6	3.7	0.98	7.7	175.5	7.7
	p4	0.71	5.0	171.3	3.7	0.89	8.3	175.3	8.4

time-averaged velocity magnitude and streamwise velocity profiles (see Figure 5). The maximum percent difference within each profile, however, was found to be as large as 96%, with median values over 20%. Thus, values at specific locations within the profile may vary considerably. The largest differences were generally seen in cross sections near the bend apex at Site 1 (S1xs2 through S1xs5), particularly at locations near the inner bank. The percent difference values for the spanwise velocity component are not reported in Table 2, due to the fact that the values were uniformly large—only two profiles have a mean percent difference less than 100%. The median value of the mean absolute difference for the spanwise velocity profiles during the mean annual flow (bankfull flow) was 0.052 m s^{-1} (0.070 m s^{-1}). These differences are the same order of magnitude as the mean spanwise velocities measured with the FV procedure. The differences in spanwise velocity are observed in both magnitude and direction (see Figures 4 and 5).

[28] Also included in Table 2 is the absolute difference between the local flow directions calculated from the FV and MV mean profiles using the Rozovskii definition. Good agreement was found for most profiles, with a median difference less than 4° for both discharges and 68% (44 out of 65) of the profiles having differences less than 5°. Despite the generally good agreement, two profiles—S1xs4p1 and S1xs4p2 during the mean annual—had absolute differences of about 40°.

4.2. Direction of Primary Flow

[29] The flow direction at each cross section is found by averaging the individual results of the four MV transects.

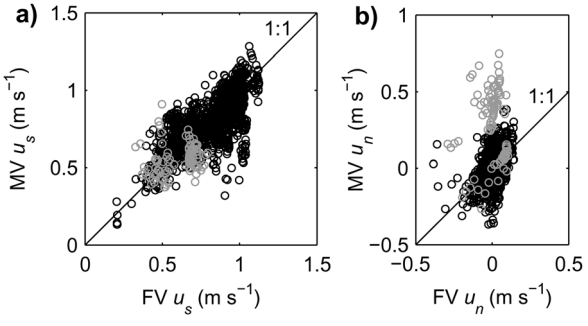

Figure 4. (a) Mean streamwise velocity and (b) mean spanwise velocity for all bins at each cross section measured with FV and MV survey procedures. The points shown in gray correspond to S1xs2p1, S1xs4p1, S1xs4p2, and S1xs4p4 during the mean annual flow.

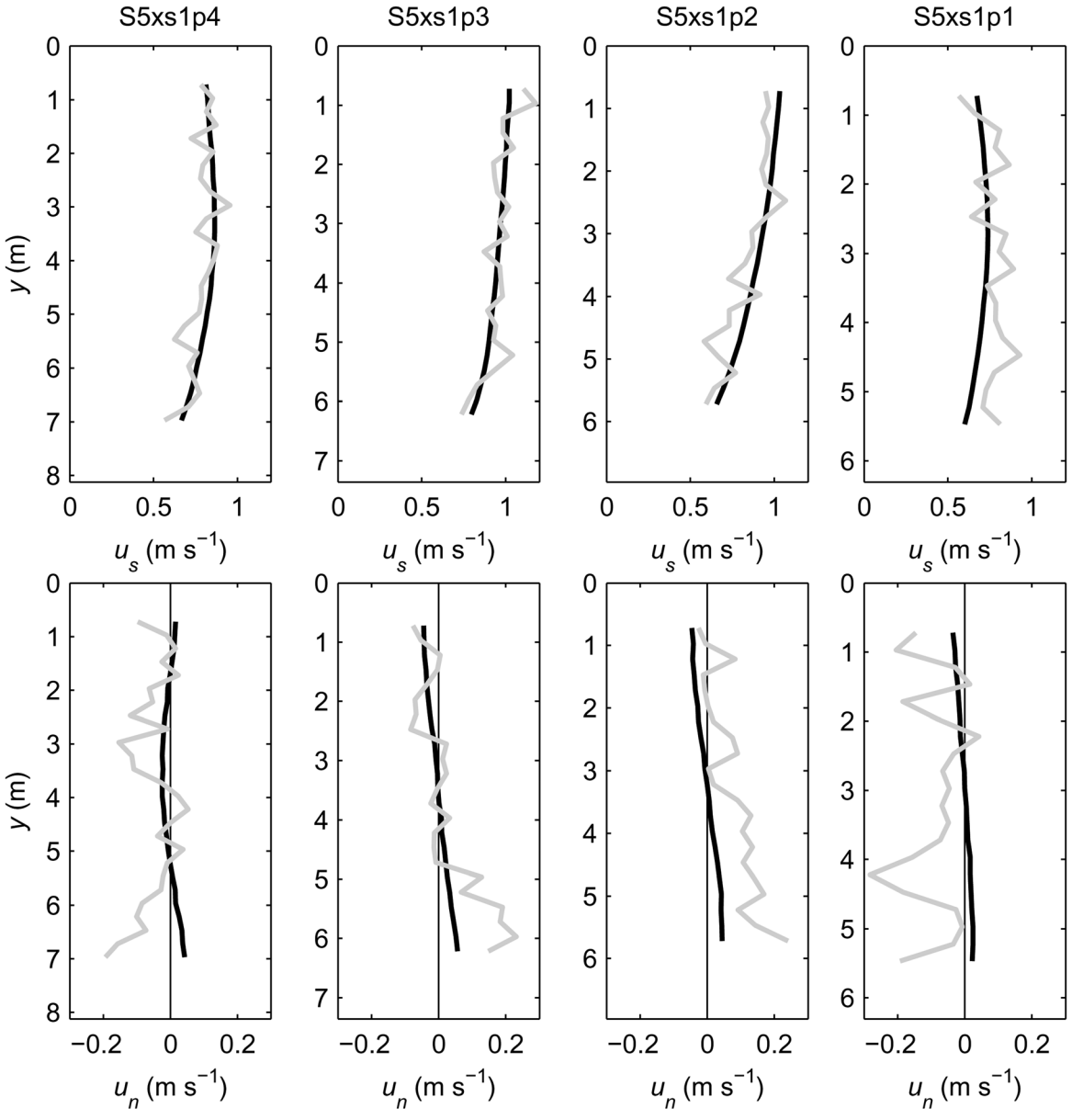

Figure 5. Streamwise and spanwise mean velocity profiles from FV (black) and MV (gray) measurements at S5xs1 during the bankfull flow.

For each transect, discharge was recomputed using the rotated velocity components and compared to the value produced by the standard equation. The mean difference between the two discharges for all transects was 2.0%. The mean flow direction along with the standard deviation and range for all cross sections are provided in Table 3. The results show good agreement among the individual transect estimates with low standard deviations and reasonable ranges considering the ADCP compass accuracy of 2° [*RD Instruments*, 2007] at all but two cross sections: S1xs4 and S1xs5 during the mean annual flow. Site and flow conditions prevented the transect boat paths from aligning with the planned path at these sites. For the majority of cross sections, an increase in discharge leads to a decrease in both the standard deviation and range, indicating a reduction in variability between the individual transect estimates. This improved agreement is likely related to the increased percentage of the flow area measured for a higher discharge. Analogous to discharge measurements, the accuracy of flow direction estimates will increase as the measured region of the channel increases. Additionally, the effect of instrument noise is reduced for larger velocities.

[30] The flow direction generally follows the channel curvature around the bend, with no significant change resulting from the increase in discharge (see Figure 2 and Table 3). The flow uniformity at the two discharges can be attributed to the fact that the flow remains within the outer bank. At bankfull discharge, however, an increased area of the inner bank is submerged. While ADCP measurements in the inner bank region were not possible due to the presence of trees and other vegetation, the flow was visually judged to be moving slowly and, thus, would contribute

Table 2. Percent Difference in Velocity and Absolute Difference in Flow Direction Between Mean Velocity Profiles Obtained From FV and MV Procedures

	Velocity Magnitude		Primary Velocity		
	Mean (%)	Maximum (%)	Mean (%)	Maximum (%)	Flow Direction
Mean annual flow					
Range	3.2–58	9.4–96	3.1–36	9.5–94	0.04°–42°
Median	10.8	20.4	11.3	23.3	3.6°
Bankfull flow					
Range	5.3–42	14.9–76	5.6–43	15.1–73	0.4°–12.7°
Median	8.6	25.6	8.9	25.3	3.3°

little to the measured discharge. These results indicate that similar flow directions are likely present for all within bank flows.

[31] The flow direction at each FV location using the Rozovskii definition is provided in Table 1. Comparing these values with the flow direction determined from the Paice definition with MV transects at each cross section gives a median difference of 2.8° (1.9°) for the mean annual (bankfull) flow. Three locations at each discharge have a difference larger than 10°, with all six measurements located at S1xs4. The greatest difference is found at S1xs4p5 during the mean annual flow—a location within a recirculation zone [see *Petrie et al*., 2013]. Table 3 provides estimates of the flow direction based on channel geometry. This geometric flow direction is found by visually positioning a spanwise axis that is perpendicular to the bank edge. The geometric flow direction remains constant for changes in discharge as a single aerial photo was used. Good agreement is seen between the flow directions determined from channel geometry and the Paice definition at all but two cross sections, S1xs3 and S1xs4. The high curvature at Site 1 directs the flow toward the outer bank in the vicinity of the apex, resulting in a flow direction from the Paice definition oriented toward the outer bank and not parallel to the banks as produced by the geometric flow direction. The effect of different definitions of flow direction on the velocity profiles is addressed in section 5.

4.3. Velocity Distribution in the Meander Bend at Site 1

4.3.1. Depth-Averaged Velocity

[32] The mean depth-averaged velocity in the streamwise flow direction using the Paice definition, U, and flow depth, H, for each FV profile is provided in Table 1. The flow depth was determined using the average of the four beam measurements over the entire sample record. For the mean annual flow (bankfull flow), U ranges from −0.02 (0.47) to 0.75 (1.06) m s^{-1}. As the flow moves through the bend, U decreases in the vicinity of the bend apex, S1xs4 and S1xs5, to accommodate the increase in flow depth. At each cross section, the maximum U value generally occurs in the outer half of the channel. The depth-averaged velocity at S1xs4p5 for the mean annual flow is a small negative value ($U = -0.02$ m s^{-1}), indicating that the mean flow is moving upstream at this location. This result suggests that this location is within a region of flow separation and recirculation as observed in both the laboratory [*Leopold et al*., 1960] and natural rivers [*Ferguson et al*., 2003]. The separation region was not captured for the bankfull flow, although a significant decrease in velocity is seen at S1xs4p5. Separation may still occur but has moved further inward, where ADCP measurements could not be obtained.

4.3.2. Primary Velocity Profiles

[33] The primary or streamwise velocity profiles for all FV measurements are shown in Figure 6. The profiles are nondimensionalized with the depth-averaged velocity and flow depth. Many of the nondimensional profiles show a similar distribution of velocity for both discharges. The largest deviation between discharges appears to occur at S1xs4. Another notable feature is the presence of a velocity dip in several profiles, particularly at locations near the banks. The velocity dip is an indicator of strong secondary velocity (see Figure 7). The primary velocity profiles at S1xs4p1 and S1xs4p2 at the bankfull flow both exhibit a sudden decrease in velocity as the free surface is approached. This behavior is due to the presence of a large tree protruding almost perpendicularly from the bank just upstream of the measurement location. At bankfull discharge, a portion of the tree is submerged. While it was not possible to determine the submerged depth of the tree, the distance is estimated to be ∼2 to 3 m based on visual observation at lower flows. The small, negative depth-averaged velocity at S1xs4p5 for the mean annual flow results in a nondimensional profile that extends over a large range with both positive and negative values. Positive values of u_s/U indicate upstream flow for the mean annual flow at S1xs4p5.

4.3.3. Secondary Velocity Profiles

[34] The mean secondary, i.e., spanwise and vertical, velocity profiles found using the flow direction determined from the MV measurements are shown in Figure 7. The velocity scale is the same for all cross sections with the exception of S1xs4. The maximum secondary velocity magnitude in each profile is typically on the order of 20% of U or less. The change in discharge produces no clear trend in the secondary velocity magnitude, with both increasing and decreasing magnitudes relative to U. The largest magnitudes of relative secondary velocity are found at S1xs4 for the mean annual flow. In particular, S1xs4p1 and S1xs4p2 have secondary velocity magnitudes close to U, while the secondary velocity magnitude at S1xs4p5 is several times larger than U.

Table 3. Direction of Primary Flow From MV Transects and Channel Geometry (°)

	Mean Annual Flow			Bankfull Flow			
	Mean	Standard Deviation	Range	Mean	Standard Deviation	Range	Channel Geometry
S1xs1	92.6	1.5	3.5	92.4	2.3	4.8	93.7
S1xs2	130.1	4.8	10.8	127.3	4.4	9.1	132.8
S1xs3	166.8	3.4	7.6	166.7	2.5	6.1	180.3
S1xs4	189.3	10.9	23.8	186.2	1.9	4.3	204.4
S1xs5	224.4	6.0	14.4	231.3	1.7	3.9	229.3
S1xs6	263.9	0.8	1.7	266.1	0.8	1.8	264.8
S5xs1	185.1	2.0	4.5	184.5	1.9	3.9	185.7
S5xs2	174.0	4.3	9.2	176.3	1.2	2.7	173.8

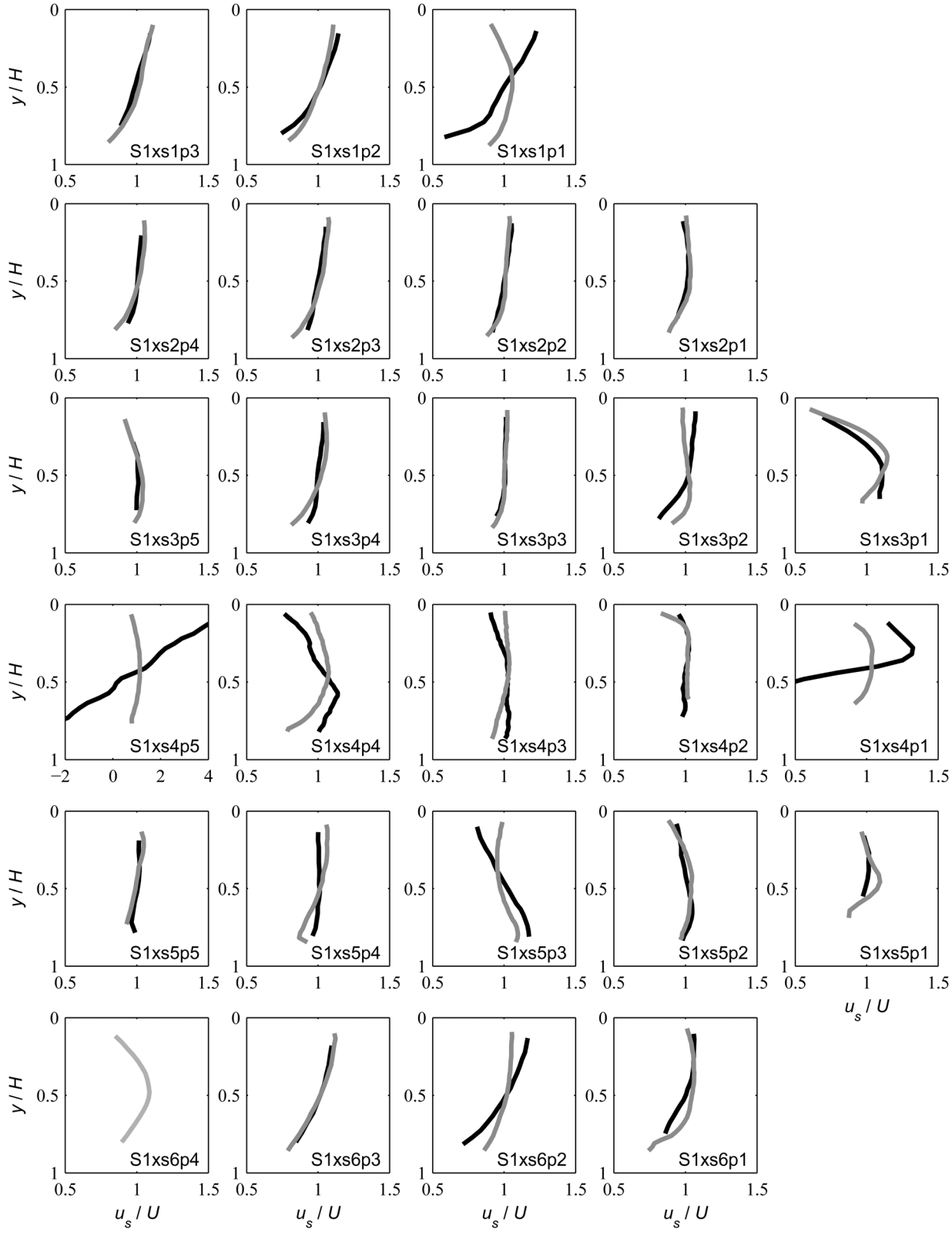

Figure 6. Mean primary velocity profiles for FV measurements at Site 1 for the mean annual flow (black) and bankfull flow (gray). Profiles location labels include the site, cross section, and profile; e.g., Site 1, cross section 2, profile 3 is notated S1xs2p3.

[35] Several well-established features of flow in natural meander bends are identified in Figure 7. A circulation cell can be seen in several profiles for both discharges at S1xs2, S1xs3, S1xs4, and S1xs6. This main circulation cell is generated by channel curvature and has been observed in both the laboratory [e.g., *Kikkawa et al.*, 1976; *Blanckaert and*

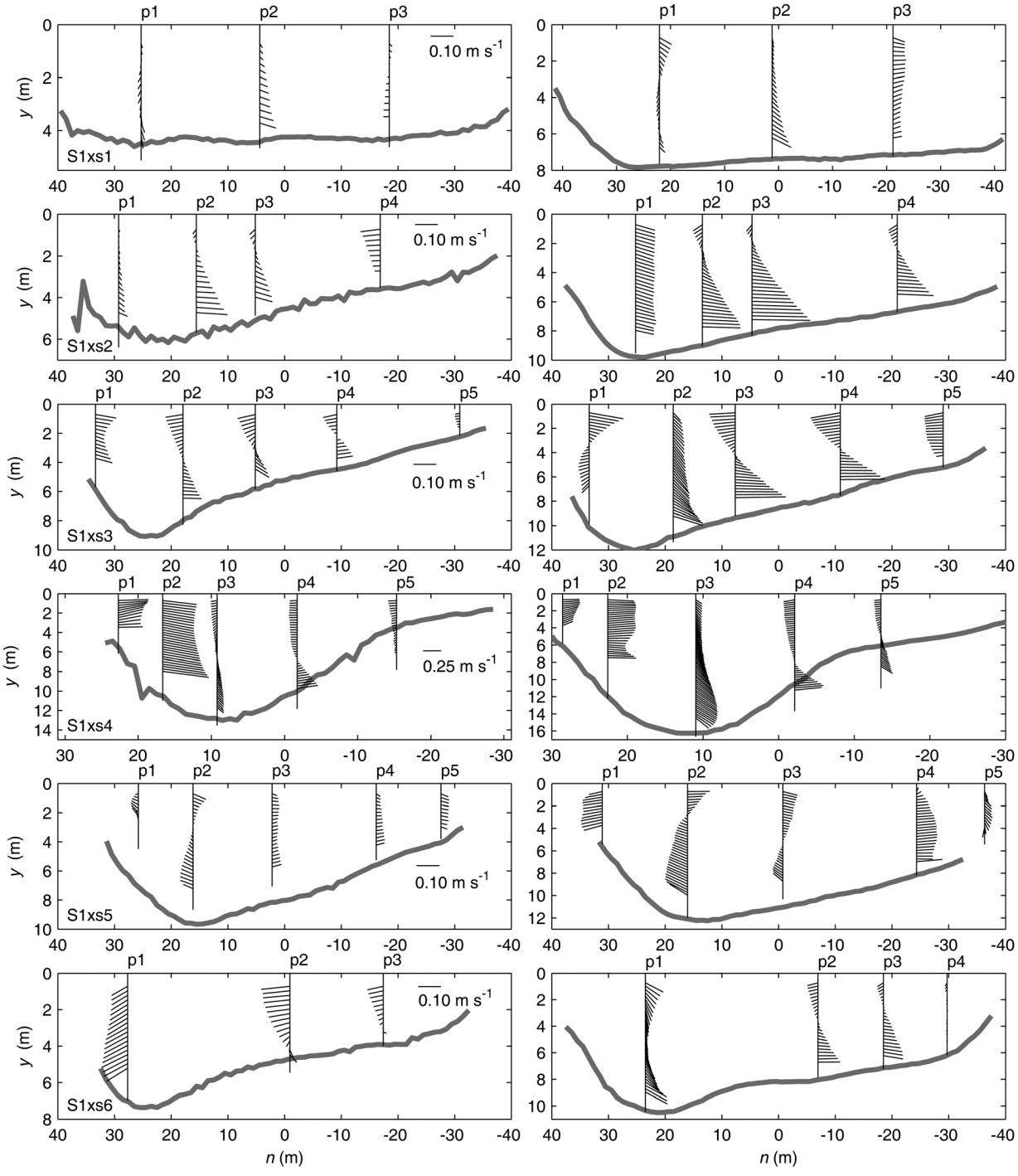

Figure 7. Mean secondary velocity profiles for FV measurements at Site 1 for the mean annual flow (left column) and bankfull flow (right column). The primary flow direction is into the page.

Graf, 2001] and field [e.g., *Thorne et al*., 1985; *Sukhodolov*, 2012]. The cell appears to move from the central region of the channel at S1xs2 to the inner half of the channel at S1xs6. It is possible that the strong negative spanwise velocities seen near the outer bank at S1xs4 may be responsible, in part, for this shift in location. Evidence of a circulation cell rotating counter to the main circulation cell is also seen near the outer bank at the apex in the profile S1xs3p1 at bankfull discharge. *Sukhodolov* [2012] observed an outer bank cell that developed near the bend apex and strengthened downstream. This outer bank cell may exist at other locations as well; however, it was not captured, due to the difficulty in obtaining measurements with the ADCP near the steep outer bank.

[36] Further effects of channel topography on the velocity field are seen at the inner bank and in the vicinity of a scour hole located just downstream of the bend apex. Topographic steering of the flow over the inner bank in the form

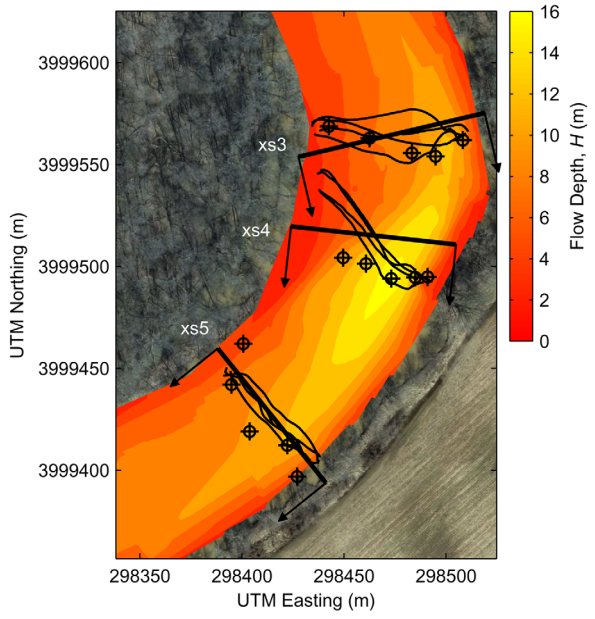

Figure 8. The FV locations (targets), boat paths for MV transects (thin lines), secondary plane orientation (thick lines), and primary flow direction (vector arrows) shown along with the measured flow depth near the apex at Site 1 for the bankfull flow.

of unidirectional positive spanwise velocities occurs in profiles for the mean annual discharge at S1xs2p4, S1xs3p5, and S1xs4p5 and for the bankfull flow at S1xs3p5. Figure 8 shows a region of increased flow depth centered approximately at S1xs4p3. Downward vertical velocities are seen in Figure 7 as the flow approaches this region in S1xs3 and S1xs4 followed by upward vertical velocities as the flow exits the scour hole at S1xs5.

5. Discussion

[37] The results from the lower Roanoke River show that spatially interpolated and averaged velocity profiles from MV transects do not adequately predict time-averaged profiles obtained from FV measurements. While general trends can be reasonably identified in the streamwise direction, agreement was poor for the spanwise velocity component. Two reasons that may explain the differences are: (1) the MV transects and FV measurements were obtained at locations with differing velocity characteristics, and (2) measurements were insufficient to describe the mean flow. *Petrie et al*. [2013] demonstrated that the FV measurements were adequate to represent the mean flow at each location and MV transects were performed while monitoring the boat path with GPS ensuring reasonable agreement among individual transect locations. When performing section straightening, however, the locations of some FV profiles were translated up to 20 m. It is possible that following translation, the FV and MV velocity data correspond to regions with different flow characteristics.

[38] The absolute difference between mean velocity components using FV and MV survey procedures and corresponding translation distance for all bins, except S1xs4p5 during the mean annual flow, are shown in Figure 9. While an increase in absolute difference with increasing translation distance is seen in some bins, the majority of bins show a similar range across all translation distances. The lack of a clear trend in absolute velocity difference with translation distance suggests that other factors, e.g., turbulence and instrument noise, play a more dominant role in producing the observed velocity difference. Figure 9 also shows that the range of the absolute difference is similar for both velocity components despite the large difference in magnitude between the two components. Additional support that the two survey procedures measured flow in similar regions of the channel is found by observing the measured flow depths. In Figure 7, the length of the line indicating the profile location corresponds to the measured flow depth from the FV measurement, while the channel boundary is the average of the flow depths measured during the MV transects. Generally, good agreement can be seen at all cross sections with the exception of S1xs4 (discussed below).

[39] For a stationary flow, the ability of a FV measurement to describe the mean flow field is controlled by the sample record length, while the number and duration of transects control the ability of the MV measurements to accurately reproduce the spatial distribution of the mean flow. *Petrie et al*. [2013] found the flow field at the lower Roanoke River study sites to be stationary for both discharges and the sample record length of 1200 s to be sufficient for all FV measurements. The four transects collected at each cross section, however, are likely not sufficient to determine the mean velocity. As the boat traverses the channel for each transect, the flow field is changing due to turbulent fluctuations. While guidelines are available for discharge [e.g., *Mueller and Wagner*, 2009], the variability in transect timing and location along with flow turbulence and instrument noise makes it difficult to prescribe a minimum number of transects required to accurately represent the spatial distribution of the mean flow. Turbulence is especially problematic when considering the secondary velocity components. Using detached-eddy simulation of a river confluence, *Tsubaki et al*. [2012] found that the maximum value of the turbulence intensity was similar for all three components. Accordingly, even if the mean values are small, sufficient individual transects are needed to ensure that these large fluctuations do not bias the resulting mean value. Previous studies comparing velocity profiles

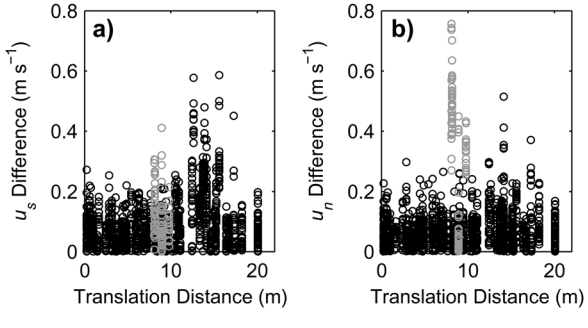

Figure 9. Absolute difference between FV and MV mean velocity for the (a) streamwise and (b) spanwise components for all bins versus translation distance. The points shown in gray correspond to the locations noted in Figure 4.

derived from transects with time-averaged values [e.g., *Muste et al*., 2004b; *Szupiany et al*., 2007] have focused on streamwise velocity or velocity magnitude and not explicitly investigated secondary velocity components. Based on the reasonable agreement of both the measured flow depths and streamwise velocity profiles using both FV and MV measurements at many locations, the likely cause of the discrepancy between FV and MV mean velocities is an insufficient number of transects at each cross section.

[40] While ADCP transects are well suited to determine flow direction with the Paice algorithm, especially when compared to point velocity measurement techniques, two issues related to the accuracy of the flow direction require further discussion. First, the flow direction is determined only by the measured region of the cross section, excluding areas near the bed, bank, and water surface. This issue applies to flow directions determined from both FV measurements using the Rozovskii definition and MV measurements applying the Paice definition. The unmeasured region near the water surface would likely have the stronger influence on the calculated flow direction as the velocity and, thus, discharge is expected to be larger than in regions close to the channel boundary. Given that the majority of the discharge is contained within the measured portion of the cross section and the difficulty in estimating vector components of velocity, it is recommended to determine the flow direction using only measured velocity data without extrapolation to unmeasured regions. The final estimate of flow direction is also dependent on the number of transects obtained at each cross section. The four transects per cross section obtained at the study sites were originally performed to measure discharge. Table 3 shows good agreement among the transects at all cross sections except S1xs4, indicating that four transects are sufficient for most cross sections at the study sites. Further study on the effect of transect number on flow direction is necessary to establish guidelines similar to those for discharge measurements [see *Mueller and Wagner*, 2009].

[41] While not investigated here, the time required to complete each transect may influence the flow direction from the Paice definition and the ability of transects to represent the mean flow. *Oberg and Mueller* [2007] found that measurement duration was more important to the accuracy of a discharge estimate than the number of transects performed. Estimates of flow direction, a bulk quantity like discharge, make likewise benefit from increased durations. Additionally, the higher spatial resolution resulting from longer duration transects may improve the ability of these transects to predict mean velocity components.

[42] The MV transects at each cross section were designed to be performed perpendicular to the banks as the channel geometry gives a first approximation of the flow direction. Perpendicular boat paths were not always possible due to difficulties maneuvering the boat, the flow conditions encountered, and other factors. Figure 8 shows the boat paths and secondary plane orientation for S1xs3 to S1xs5 during the bankfull flow. While reasonable agreement between the boat paths and secondary plane are seen at S1xs3 and S1xs5, significant differences occur at S1xs4. An area of vegetation near the inner bank not visible in the aerial photograph forced the boat paths to diverge from the planned course. This region shows spatial variability in channel topography and likely flow characteristics as well. The variability in topography can be seen in Figure 7 by examining the flow depths measured with FV and MV procedures at S1xs4p4 and S1xs4p5. The difference in the boat paths and the FV measurement locations along with the changes in bathymetry suggest that the MV transects and FV measurements at S1xs4p4 and S1xs4p5 are measuring regions where the flow may not be considered homogeneous. Whenever possible, the location of a cross section should be selected so that sufficient boat access is available to perform transects.

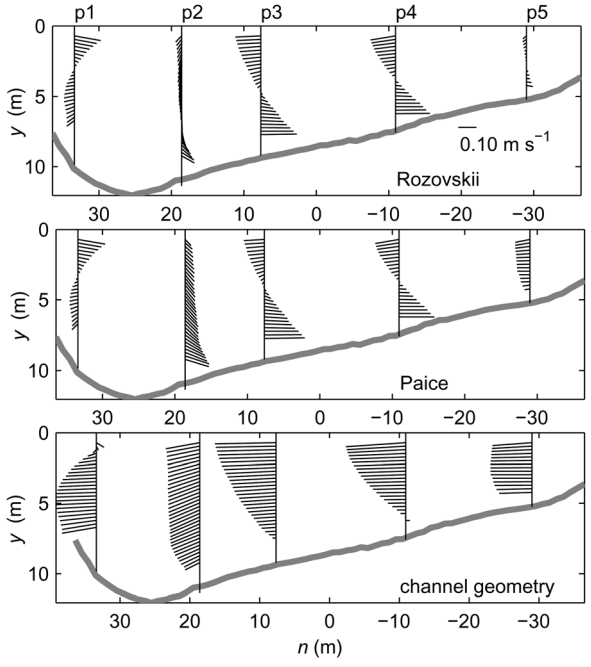

Figure 10. Secondary velocity profiles at S1xs3 for the bankfull flow using different definitions for the flow direction. The primary flow direction is into the page.

[43] The different definitions of the primary flow direction all provide a means to visualize three-dimensional velocity data in an orthogonal coordinate system. Figure 10 shows the mean secondary velocity profiles at S1xs3 for the bankfull flow considering three different definitions: (1) Rozovskii, (2) Paice, and (3) channel geometry. As noted previously, the Rozovskii definition produces a flow direction for each profile (see Table 1), making the presentation of velocity in Figure 10 somewhat misleading. At this cross section, the range of flow directions from the Rozovskii definition is 9.4°, with a mean value close to the primary flow direction determined with the Paice definition. Despite this agreement, differences in the secondary velocity patterns are seen in two profiles: S1xs3p2 and S1xs3p5. The flow direction based on the channel geometry differs from that of the Paice definition by more than 10°. The strong curvature of the meander bend directs the flow toward the outer bank in the vicinity of the apex, as shown in Figures 2 and 8. By not considering the flow conditions, the channel geometry definition results in a significantly different pattern of secondary velocity. The spanwise component using the channel geometry definition is directed almost entirely toward the outer bank, obscuring the

circulation pattern observed with the Paice definition. The results presented in Figure 10 highlight two advantages of the Paice definition when presenting secondary velocity profiles at a cross section: (1) the velocity at each profile occurs in the plane as shown and (2) the orientation of the secondary plane is determined by the flow characteristics at the site, clarifying secondary velocity patterns of small magnitude and removing the need for decisions regarding channel orientation. The fact that both cross sections at Site 5 show similar secondary velocity profiles with the Paice and channel geometry definitions for both discharges demonstrates that results of the two definitions diverge as channel curvature increases.

6. Conclusions

[44] A methodology has been proposed to quantify the mean 3-D velocity distribution in natural rivers using a boat-mounted ADCP. The approach benefits from the advantages of the different survey procedures. The high spatial resolution of MV transects define the coordinate system for cross sections and establish the cross section bathymetry. FV measurements obtained along the cross section provide mean 3-D velocity profiles at discrete locations. The methodology can be adapted to present spatially averaged velocity from MV measurements and time-averaged velocity from FV measurements in the stream-based coordinate system. Comparing 65 mean velocity profiles obtained with both FV and MV procedures demonstrates that MV transects can often provide reasonable estimates of velocity magnitude profiles, streamwise velocity profiles, and local flow direction. The spanwise velocity profiles from the two survey procedures show sizeable differences, likely stemming from the inability of the four transects obtained at each cross section to adequately represent secondary velocity. This comparison demonstrates the need for high temporal resolution FV measurements to quantify mean secondary velocity components. Applying the methodology to a meander bend, several well-known flow features are captured, including a main circulation cell, an outer-bank circulation cell, unidirectional flow over the inner bank, and separation at the inner bank.

[45] The orientation of the coordinate system is specified with the Paice definition, which has several advantageous characteristics. The flow direction is constant for a cross section, allowing secondary velocity to be visualized in a single plane defined by the spanwise and vertical axes. Additionally, flow characteristics determine the flow direction, removing the uncertainty associated with geometric approaches to defining the flow direction in natural channels. The presentation of velocity data along cross section allows the field data to be integrated with numerical models to provide boundary conditions, calibration data, and validation data.

[46] While the procedure performs well for the conditions encountered at the study site, further testing should be undertaken for a variety of flow conditions and channel geometries. For example, the procedure could be expanded to confluences where individual flow directions are computed from each tributary, following the recommendation of *Lane et al*. [2000]. Studies at confluences and other complex flows may require further investigation of the effects of repeat transects and transect duration on the average flow direction.

Appendix A: Derivation of Equations to Calculate Discharge

[47] Applying the Paice definition to MV transects requires that the streamwise or spanwise discharge be calculated for a specified angle of rotation. While the equations developed here are necessary to apply the Paice method, they are not meant to replace the traditional discharge calculation method. Derivations of the equation used to calculate the total discharge from a MV transect can be found in *Christensen and Herrick* [1982] and *Simpson and Oltmann* [1993]. Derivation of the equation for the discharge in the streamwise flow direction is demonstrated and a similar procedure may be followed for the spanwise discharge. Discharge in a river is defined as

$$Q = \iint_A V \bullet n dA, \tag{A1}$$

where Q is the discharge across the surface A, $\mathbf{V}$ is the velocity vector of the river flow, $\mathbf{n}$ is the normal vector to A, and dA is the differential area of A. The surface A is specified by the angle of rotation and is the plane defined by the two axes mutually orthogonal to the primary flow direction as shown in Figure A1, i.e., the spanwise, n, and vertical, z, axes. By definition, A is perpendicular to the streamwise axis and, therefore, $\mathbf{n}$ is constant. The integrand in equation (A1) becomes

$$\mathbf{V} \bullet \mathbf{n} = u_s, \tag{A2}$$

where u_s is the streamwise component of velocity. The differential area can be rewritten as

$$dA = dndz, \tag{A3}$$

where dn is the differential distance along the spanwise axis and dz is the differential distance along the vertical axis. The distance dn is found by projecting the boat path onto the plane A using the boat velocity in stream coordinates (see Figure A1),

$$dn = V_{bn} dt, \tag{A4}$$

where V_{bn} is the spanwise component of the boat velocity and dt is the differential elapsed time. Substituting equations (A2), (A3), and (A4) into equation (A1) yields the general equation for the discharge in the primary flow direction:

$$Q_s = \int_0^T \int_0^H u_s V_{bn} dz dt, \tag{A5}$$

where T is the total elapsed time for the transect and H is the flow depth. The discrete form of equation (A5) is better suited for ADCP data. Following a similar approach to that

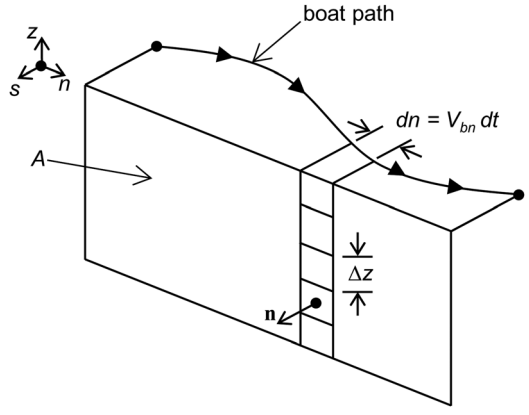

Figure A1. Definition sketch for calculating discharge in stream coordinates.

presented by *Simpson* [2001, pp. 27–29], the discharge in the primary flow direction for the *i*th ensemble is

$$Q_{si} = \sum_{j}^{m} u_{sj}(V_{bn})_i \Delta t_i \Delta z, \tag{A6}$$

where the ensemble contains $j = 1, 2, \ldots, m$ bins, u_{sj} is the primary velocity component of the *j*th bin, $(V_{bn})_i$ is the spanwise component of the boat velocity of the ensemble, Δz is the bin size, and Δt_i is the time elapsed between ensembles i and $i-1$. Summing over all ensembles provides the total discharge in the primary direction:

$$Q_s = \sum_{i}^{k} Q_{si}, \tag{A7}$$

where the transect contains $i = 1, 2, \ldots, k$ ensembles. Following a similar procedure, the discharge in the secondary direction for the *i*th ensemble and the total secondary discharge are calculated with equations (1) and (2).

Notation

H	flow depth (m).
$\mathbf{n}$	unit normal vector.
Q	discharge ($m^3\ s^{-1}$).
Q_n	discharge in the spanwise direction ($m^3\ s^{-1}$).
Q_s	discharge in the streamwise direction ($m^3\ s^{-1}$).
u_n	spanwise velocity ($m\ s^{-1}$).
u_s	streamwise velocity ($m\ s^{-1}$).
U	depth-averaged streamwise velocity ($m\ s^{-1}$).
$\mathbf{V}$	river velocity vector ($m\ s^{-1}$).
V_n	spanwise boat velocity ($m\ s^{-1}$).
V_s	streamwise boat velocity ($m\ s^{-1}$).
y	depth below water surface (m).
α	streamwise flow direction (°).
Δt	time elapsed between ensembles (s).
Δz	bin size (m).

[48] **Acknowledgments.** The authors acknowledge the financial support of Dominion, the U.S. Army Corps of Engineers, the Hydro Research Foundation, and the Edna Bailey Sussman Foundation. Ozan Celik and Nikos Apsilidis assisted with the field measurements. Bob Graham graciously provided a boat when engine trouble threatened to cut our field campaign short. The comments and criticisms of three anonymous reviewers and the Associate Editor have improved the presentation of this work.

References

Blanckaert, K. (2011), Hydrodynamic processes in sharp meander bends and their morphological implications, *J. Geophys. Res.*, *116*, F01003, doi:10.1029/2010JF001806.

Blanckaert, K., and W. H. Graf (2001), Mean flow and turbulence in open-channel bend, *J. Hydraul. Eng.*, *127*(10), 835–847.

Christensen, J. L., and L. E. Herrick (1982), Mississippi River test, Final Rep. DCP4400/300, vol. *1*, prepared by AMETEK for U.S. Geol. Surv., El Cajon, Calif.

De Vriend, H. J. (1979), Flow measurements in a curved rectangular channel, Internal Rep. 9–79, Delft Univ. of Technol., Delft, Netherlands.

Dietrich, W. E., and J. D. Smith (1983), Influence of the point-bar on flow through curved channels, *Water Resour. Res.*, *19*(5), 1173–1192.

Dinehart, R. L., and J. R. Burau (2005), Averaged indicators of secondary flow in repeated acoustic Doppler current profiler crossings of bends, *Water Resour. Res.*, *41*, W09405, doi:10.1029/2005WR004050.

Ferguson, R. I., D. R. Parsons, S. N. Lane, and R. J. Hardy (2003), Flow in meander bends with recirculation at the inner bank, *Water Resour. Res.*, *39*(11), 1322, doi:10.1029/2003WR001965.

Gordon, R. L. (1989), Acoustic measurement of river discharge, *J. Hydraul. Eng.*, *115*(7), 925–936.

Guerrero, M., and A. Lamberti (2011), Flow field and morphology mapping using ADCP and multibeam techniques: Survey in the Po River, *J. Hydraul. Eng.*, *137*(12), 1576–1587, doi:10.1061/(ASCE)HY.1943–7900.0000464.

Hey, R. D., and P. C. B. Rainbird (1996), Three-dimensional flow in straight and curved reaches, in *Advances in Fluvial Dynamics and Stratigraphy*, edited by P. A. Carling and M. R. Dawson, pp. 33–66, John Wiley, Chichester, U. K.

Hupp, C. R., E. R. Schenk, J. M. Richter, R. K. Peet, and P. A. Townsend (2009), Bank erosion along the dam-regulated lower Roanoke River, North Carolina, in *Management and Restoration of Fluvial Systems with Broad Historical Changes and Human Impacts, Geological Society of America Special Papers 451*, edited by L. A. James, S. L. Rathburn, and G. R. Whittecar, p. 97–108, Geological Society of America, Boulder, Colo., doi:10.1130/2009.2451(06).

Jamieson, E. C., C. D. Rennie, R. B. Jacobson, and R. D. Townsend (2011), 3-D flow and scour near a submerged wing dike: ADCP measurements on the Missouri River, *Water Resour. Res.*, *47*, W07544, doi:10.1029/2010WR010043.

Kikkawa, H., S. Ikeda, and A. Kitagawa (1976), Flow and bed topography in curved open channels, *J. Hydraul. Eng.*, *102*(9), 1327–1342.

Lane, S. N., K. F. Bradbrook, K. S. Richards, P. M. Biron, and A. G. Roy (2000), Secondary circulation cells in river channel confluences: Measurement artefacts or coherent flow structures?, *Hydrol. Processes*, *14*(11-12), 2047–2071.

Leopold, L. B., R. A. Bagnold, M. G. Wolman, and J. L. M. Brush (1960), Flow resistance in sinuous or irregular channels, U.S. Geol. Surv. Prof. Pap. 282-D.

Markham, A. J., and C. R. Thorne (1992), Geomorphology of gravel-bed river bends, in *Dynamics of Gravel-Bed Rivers*, edited by P. Billi et al., pp. 433–450, John Wiley, Chichester, U. K.

Mueller, D. S., and C. R. Wagner (2009), Measuring discharge with acoustic Doppler current profilers from a moving boat, U.S. Geol. Surv. Tech. and Methods 3A-22.

Muste, M., K. Yu, T. Pratt, and D. Abraham (2004a), Practical aspects of ADCP data use for quantification of mean river flow characteristics; part II: Fixed-vessel measurements, *Flow Meas. Instrum.*, *15*(1), 17–28, doi:10.1016/j.flowmeasinst.2003.09.002.

Muste, M., K. Yu, and M. Spasojevic (2004b), Practical aspects of ADCP data use for quantification of mean river flow characteristics; part 1: Moving-vessel measurements, *Flow Meas. Instrum.*, *15*(1), 1–16, doi:10.1016/j.flowmeasinst.2003.09.001.

Nam, S., M. Gutierrez, P. Diplas, J. Petrie, A. Wayllace, N. Lu, and J. J. Munoz (2010), Comparison of testing techniques and models for establishing the SWCC of riverbank soils, *Eng. Geol.*, *110*(1-2), 1–10, doi:10.1016/j.enggeo.2009.09.003.

Nam, S., M. Gutierrez, P. Diplas, and J. Petrie (2011), Determination of the shear strength of unsaturated soils using the multistage direct shear test, *Eng. Geol.*, *122*(3–4), 272–280, doi:10.1016/j.enggeo.2011.06.003.

Nanson, R. A. (2010), Flow fields in tightly curving meander bends of low width-depth ratio, *Earth Surf. Processes Landforms*, *35*(2), 119–135, doi:10.1002/esp.1878.

Oberg, K., and D. S. Mueller (2007), Validation of streamflow measurements made with acoustic Doppler current profilers, *J. Hydraul. Eng.*, *133*(12), 1421–1432, doi:10.1061/(ASCE)0733–9429(2007)133:12(1421).

Paice, C. (1990), Hydraulic control of river bank erosion: An environmental approach, PhD thesis, Sch. of Environ. Sci., Univ. of East Anglia, Norwich, U. K.

Petrie, J., P. Diplas, M. Gutierrez, and S. Nam (2013), Data evaluation for acoustic Doppler current profiler measurements obtained at fixed locations in a natural river, *Water Resour. Res.*, *49*, 1–14, doi:10.1002/wrcr.20112.

RD Instruments (2007), *Work Horse Rio Grande Acoustic Doppler Current Profiler Technical Manual*, San Diego, Calif.

Rennie, C. D., and M. Church (2010), Mapping spatial distributions and uncertainty of water and sediment flux in a large gravel bed river reach using an acoustic Doppler current profiler, *J. Geophys. Res.*, *115*, F03035, doi:10.1029/2009JF001556.

Rennie, C. D., R. G. Millar, and M. A. Church (2002), Measurement of bed load velocity using an acoustic Doppler current profiler, *J. Hydraul. Eng.*, *128*(5), 473–483.

Rozovskii, I. L. (1957), Flow of water in bends of open channels [in Russian], Acad. of Sci. of the Ukrainian SSR, Kiev. (English translation, Isr. Program for Sci. Transl., Jerusalem, 1961.).

Rüther, N., J. Jacobsen, N. R. B. Olsen, and G. Vatne (2010), Prediction of the three-dimensional flow field and bed shear stresses in a regulated river in mid-Norway, *Hydrol. Res.*, *41*(2), 145–152, doi:10.2166/nh.2010.064.

Shen, Y., and P. Diplas (2008), Application of two-and three-dimensional computational fluid dynamics models to complex ecological stream flows, *J. Hydrol.*, *348*(1-2), 195–214, doi:10.1016/j.jhydrol. 2007.09.060.

Shen, Y., and P. Diplas (2010), Modeling unsteady flow characteristics of hydropeaking operations and their implications on fish habitat, *J. Hydraul. Eng.*, *136*(12), 1053–1066, doi:10.1061/(ASCE)HY.1943–7900.0000112.

Simpson, M. R. (2001), Discharge measurements using a broad-band acoustic Doppler current profiler, U.S. Geol. Surv. Open File Rep. 01-1, 123 pp., Sacramento, Calif.

Simpson, M. R., and R. N. Oltmann (1993), Discharge-measurement system using an acoustic Doppler current profiler with applications to large rivers and estuaries, U.S. Geol. Surv. Water Supply Pap. 2395, 32 pp.

Sukhodolov, A. N. (2012), Structure of turbulent flow in a meander bend of a lowland river, *Water Resour. Res.*, *48*, W01516, doi:10.1029/2011WR010765.

Szupiany, R. N., M. L. Amsler, J. L. Best, and D. R. Parsons (2007), Comparison of fixed- and moving-vessel flow measurements with an aDp in a large river, *J. Hydraul. Eng.*, *133*(12), 1299–1309, doi:10.1061/(ASCE)0733–9429(2007)133:12(1299).

Thorne, C. R., L. W. Zevenbergen, J. C. Pitlick, S. Rais, J. B. Bradley, and P. Y. Julien (1985), Direct measurements of secondary currents in a meandering sand-bed river, *Nature*, *315*(6022), 746–747.

Tominaga, A., I. Nezu, K. Ezaki, and H. Nakagawa (1989), Three-dimensional turbulent structure in straight open channel flows, *J. Hydraul. Res.*, *27*(1), 149–173.

Tsubaki, R., Y. Kawahara, Y. Muto, and I. Fujita (2012), New 3-D flow interpolation method on moving ADCP data, *Water Resour. Res.*, *48*, W05539, doi:10.1029/2011WR010867.